Structural investigations on diorgano- and triorganotin(IV) derivatives of [*meso*-tetra(4-sulfonatophenyl)porphine] metal chlorides

C. Pellerito [a], M. Scopelliti [a], T. Fiore [a], L. Nagy [b], G. Barone [a], M. Abbate [a], G.C. Stocco [a], L. Pellerito [a,*]

[a] *Dipartimento di Chimica Inorganica e Analitica "Stanislao Cannizzaro", Università di Palermo, Viale delle Scienze, Parco d'Orleans II, 90128 Palermo, Italy*
[b] *Department of Inorganic and Analytical Chemistry, University of Szeged, P.O. Box 440, H-6701 Szeged, Hungary*

Abstract

Several new complexes of organotin(IV) moieties with MCl_n[*meso*-tetra(4-sulfonatophenyl)porphine], $(R_2Sn)_2MCl_n$[*meso*-tetra(4-sulfonatophenyl)-porphinate]s and $(R_3Sn)_4MCl_n$ [*meso*-tetra(4-sulfonatophenyl)porphinate]s, [M = Fe(III), Mn(III): $n = 1$, R = Me, *n*-Bu; Ph; M = Sn(IV): $n = 2$, R = Me, *n*-Bu] have been synthesized and their solid state configuration investigated by infrared (IR) and Mössbauer spectroscopy, and by ^1H and ^{13}C NMR in D_2O.

The electron density on the metal ion coordinated inside the porphyrin ring is not influenced by the organotin(IV) moieties bonded to the oxygen atoms of the side chain sulfonatophenyl groups, as it has been inferred on the basis of Mössbauer spectroscopy and, in particular, from the invariance of the isomer shift of the Fe(III) and Sn(IV) atoms coordinated into the porphyrin square plane of the newly synthesized complexes, with respect to the same atoms in the free ligand.

As far as the coordination polyhedra around the peripheral tin atoms are concerned, infrared spectra and experimental Mössbauer data would suggest octahedral and trigonal bipyramidal environments around tin, in polymeric configurations obtained, respectively, in the diorganotin derivatives through chelating or bridging sulfonate groups coordinating in the square plane, and in triorganotin(IV) complexes through bridging sulfonate oxygen atoms in axial positions.

The structures of the $(Me_3Sn)_4Sn(IV)Cl_2$[*meso*-tetra(4-sulfonatophenyl)porphinate] and of the two model systems, $Me_3Sn(PS)(HPS)$ and $Me_2Sn(PS)_2$ [HPS = phenylsulfonic acid], have been studied by a two layer ONIOM method, using the hybrid DFT B3LYP functional for the higher layer, including the significant tin environment. This approach allowed us to support the structural hypotheses inferred by the IR and Mössbauer spectroscopy analysis and to obtain detailed geometrical information of the tin environment in the compounds investigated.

^1H and ^{13}C NMR data suggested retention of the geometry around the tin(IV) atom in D_2O solution.
© 2005 Elsevier B.V. All rights reserved.

Keywords: Organotin(IV); Porphinate; Infrared; Mössbauer; DFT calculations; ^1H and ^{13}C NMR

1. Introduction

In the recent past, in spite of the number of publications which appeared in the literature on the chemistry of metal porphyrins, only few papers dealt with side chain derivatives of metallic or organometallic moieties. Bis[diorganotin(IV)chloro]-protoporphyrin IX complexes have been investigated in the solid and in solution phase [1], and chromosome damages have been evidenced in early-developing embryos of *Anilocra physodes* L. (Crustacea, Isopoda) following exposure to bis(dimethyltin(IV)chloro)-protoporphyrin IX [2]. Fifteen side chain platinum(II)-porphyrin

---

* Corresponding author. Tel.: +39 091 590367; fax: +39 091 427584.
E-mail address: bioinorg@unipa.it (L. Pellerito).

complexes have been synthesized, chemically characterized and their antitumor activity in vivo towards MDA-MB 231 mammary carcinoma cell line tested [3].

A series of mono-, bis- and tetrakisporphyrin assemblies have been prepared, by Yuan et al. [4], from interaction of Zn(II)[5-(*p*-pyridyl)-10,15,20-triphenylporphyrinate] and Zn(II)[5-(*p*-pyridyl)-10,15,20-tri(*p*-tolyl)porphyrinate] with *trans*-Pd(DMSO)$_2$Cl$_2$ and *cis*-Pt(DMSO)$_2$Cl$_2$. In all the synthesized complexes, both Pd and Pt were side chain coordinated to the nitrogen donor atom of the pyridyl groups [4].

[*meso*-Tetra(4-carboxyphenyl)porphine] (=H$_6$TPPC) and [*meso*-tetra(4-sulfonatophenyl) porphine] (=H$_6$TPPS) interaction with diorgano and triorganotin(IV) moieties have been investigated and the obtained results evidenced the formation of complexes with formula (R$_2$Sn)$_2$H$_2$-TPPC, (R$_3$Sn)$_4$H$_2$TPPC, (R$_2$Sn)$_2$H$_2$TPPS and (R$_3$Sn)$_4$H$_2$-TPPS (R = Me, *n*-Bu, Ph), respectively. Their solid state and solution configurations were reported, together with their in vivo cytotoxic activity [5,6]. Stepwise assembly of unsymmetrical supramolecular arrays containing *meso*-4′-pyridylphenylporphyrins and ruthenium coordination compounds, have been reported [7,8]. Recently, a paper dealing with diorganotin(IV) and triorganotin(IV) derivatives of chlorin-e$_6$ (organo = Me, *n*-Bu, Ph), their effect on sea urchin embryonic development and induced apoptosis, has been published [9]. Finally, in order to examine the pathway with which (Bu$_2$Sn)$_2$TPPS and (Bu$_3$Sn)$_4$TPPS induced A375 cell death, DNA fragmentation analysis, Annexin V binding and PI uptake as well as caspases activation analysis by Western blot, were carried out [10].

In the present paper, investigations have been extended to di- and triorganotin(IV) complexes of *meso*-tetra(4-sulfonatophenyl)porphine derivatives, containing Fe(III)Cl, Mn(III)Cl or Sn(IV)Cl$_2$ groups within the porphyrin ring (Fig. 1a and b).

2. Experimental

2.1. Chemical materials and methods

R$_2$SnO (R = Me, *n*-Bu, Ph), (*n*-Bu$_3$Sn)$_2$O and Ph$_3$SnOH used in the syntheses, were freshly prepared by hydrolysis of the parent organotin(IV)chloride (Fluka, Bucks, Switzerland) and recrystallized from benzene, while Me$_3$SnOH was a Alfa Aesar product (Johnson Matthey GmbH, Karlsruhe, Germany). The free Fe(III)ClH$_4$[*meso*-tetra-(4-sulfonatophenyl)porphinate], Mn(III)ClH$_4$[*meso*-tetra-(4-sulfonatophenyl)porphinate] and Sn(IV)Cl$_2$H$_4$[*meso*-tetra(4-sulfonatophenyl)porphinate] ligands (Fig. 1a and b) were Porphyrin Products (Logan, UT, USA).

(R$_2$Sn)$_2$MCl$_n$[*meso*-tetra(4-sulfonatophenyl)porphinate]s and (R$_3$Sn)$_4$MCl$_n$[*meso*-tetra(4-sulfonatophenyl)porphinate]s, (M = Fe(III), Mn(III): n = 1, R = Me, *n*-Bu; Ph; M = Sn(IV): n = 2, R = Me, *n*-Bu), have been obtained according to the following procedures.
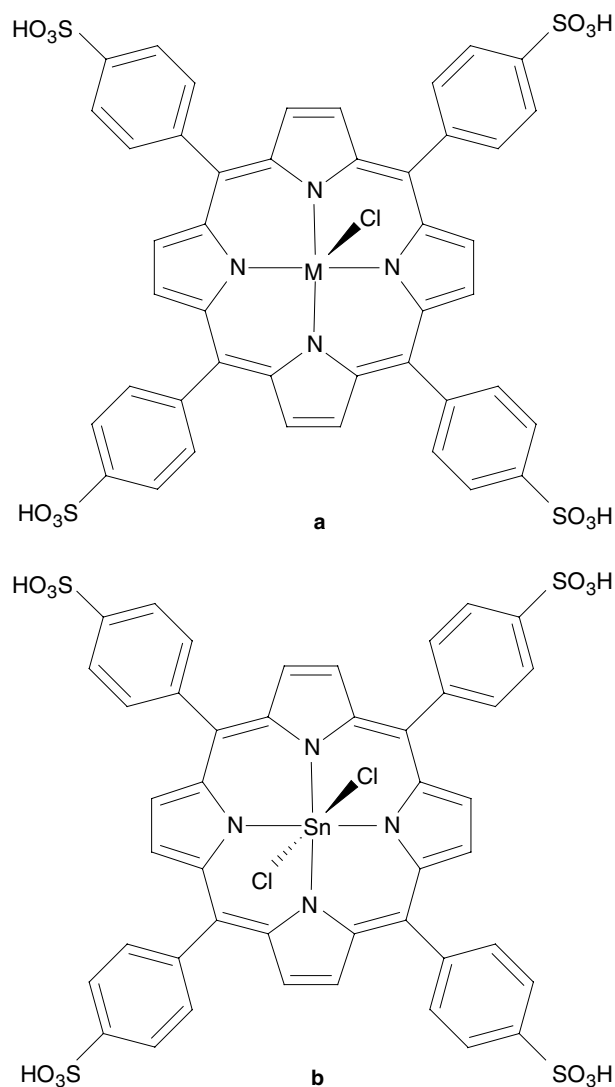

Fig. 1. M(III)Cl[*meso*-tetra(4-sulfonatophenyl)porphine], [M = Fe(III), Mn(III)] (a); Sn(IV)Cl$_2$[*meso*-tetra(4-sulfonatophenyl)porphine] (b).

2.1.1. (R$_2$Sn)$_2$MCl$_n$[meso-tetra(4-sulfonatophenyl)-porphinate]s, [M = Fe(III), Mn(III): n = 1, R = Me, n-Bu; Ph; M = Sn(IV): n = 2, R = Me, n-Bu]

MCl$_n$H$_4$[*meso*-tetra(4-sulfonatophenyl)porphine] and the appropriate (R$_2$Sn)$_2$O, suspended in 50 ml of CH$_3$OH, in the 1:2 stoichiometric ratio, were allowed to react for 24 h at about 40 °C, under a constant stirring. The brown solid (R$_2$Sn)$_2$MCl$_n$[*meso*-tetra(4-sulfonatophenyl)porphinate]s, which precipitated on cooling, were recovered, recrystallized from methanol and dried over P$_4$O$_{10}$.

2.1.2. (R$_3$Sn)$_4$MCl$_n$[meso-tetra(4-sulfonatophenyl)-porphinate]s, [M = Fe(III), Mn(III): n = 1, R = Me, n-Bu; Ph; M = Sn(IV): n = 2, R = Me]

MCl$_n$H$_4$[*meso*-tetra(4-sulfonatophenyl)porphine] were allowed to react into 50 ml of CH$_3$OH, for 24 h at about 40 °C, under a constant stirring, together with the stoichiometric amount of Me$_3$SnOH, (Bu$_3$Sn)$_2$O or Ph$_3$SnOH. The brown solid (R$_3$Sn)$_4$MCl$_n$[*meso*-tetra(4-sulfonatophe-

nyl)porphinate]s obtained were recovered by filtration, recrystallized from methanol and dried over P_4O_{10} under vacuum.

The recrystallized solids were analyzed for C, H, N, S contents (Table 1), by using a Vario EL III CHNS elemental analyzer (Elementar Analysensysteme GmbH, Hanau, Germany).

Thermogravimetric (TG) measurements were carried out from room temperature (= RT) up to 600 °C, with a Mettler TA-300 system operating in a pure nitrogen atmosphere, in alumina crucible and at a heating rate of 5 °C/min, using alumina as reference. The organotin(IV)MCl$_n$- [meso-tetra(4-sulfonatophenyl)porphinate] complexes had a characteristic thermal decomposition pattern, between 60 and 110 °C, due to loss of six water molecules (Table 1). The experimental results and in particular the temperature at which the water molecules have been lost, should exclude any involvement in coordination sphere of the tin atom.

FT-IR spectra (Table 2) were registered, as nujol and hexachlorobutadiene mulls, on a Mod. Spectrum one Perkin–Elmer FT-IR, between CsI windows, in the 4000–250 cm^{-1} region.

^{1}H and ^{13}C NMR spectra of non-paramagnetic organotin(IV) derivatives were recorded on a Bruker AC 250E instrument, operating at 63 and 250 MHz, respectively, using DMSO as solvent and tetramethylsilane (TMS) as internal reference; using D_2O as solvent, DSS [= 3-(trimethylsilyl)-1-propanesulfonic acid sodium salt] has been used as external reference (Tables 6 and 7).

The ^{119}Sn Mössbauer spectra (Table 3) were measured at liquid nitrogen temperature with a multichannel analyzer [TAKES Mod. 269, Ponteranica, Bergamo (Italy)] and the following Wissenschaftliche Elektronik system [MWE, München (Germany)]: an MR250 driving unit, an FG2 digital function generator and an MA250 velocity transducer, moved at linear velocity, constant acceleration, in a triangular waveform. The organotin(IV) samples were maintained at liquid nitrogen temperature in a model NDR-1258-MD Cryo liquid nitrogen cryostat (Cryo Industries of America, Inc., Atkinson, NH, USA) with a Cryo sample holder. The 77.3 ± 0.1 K temperature was controlled with a model ITC 502 temperature controller of the Oxford Instruments (Oxford, England). The multichannel calibration was performed with an enriched iron foil [^{57}Fe = 95.2%, thickness 0.06 mm, Dupont, MA (USA)], at room temperature, by using a ^{57}Co–Pd source [(10 mCi, Ritverc GmbH, St. Petersburg (Russia)], while the zero point of the Doppler velocity scale has been determined, at room temperature, through absorption spectra of natural $CaSnO_3$ (^{119}Sn = 0.5 mg/cm^2) and a $Ca^{119}SnO_3$ source [10 mCi, Ritverc GmbH, St. Petersburg (Russia)]. The obtained $5 \cdot 10^5$ count spectra were refined, to obtain the isomer shift, δ (mm s^{-1}), and the nuclear quadrupole splitting, $|\Delta_{exp}|$ (mm s^{-1}), values reported in Table 3.

2.2. Quantum chemical calculations

Two layers ONIOM calculations [11], with full geometry optimization, were performed on the structure of $(Me_3Sn)_4Sn(IV)Cl_2TPPS$, as well as of $Sn(IV)Cl_2H_4TPPS$ and $(Me_3Sn)_4H_2TPPS$, for comparison purposes, and on the two model complexes of trimethyltin(IV) and dimethyltin(IV) with the ligand phenylsulfonic acid (HPS), $Me_3Sn(PS)(HPS)$ and $Me_2Sn(PS)_2$. The density functional theory (DFT) hybrid Becke's three-parameter method (B3LYP) level, with the double-zeta valence plus polarization (DZVP) basis set [12], was used for the higher layer, including the tin-dichloride protoporphyrin environment or the di- or trimethyltin(IV)-sulfonate environment, respectively; the semiempirical AM1 method was used for the lower layer. All calculations were performed by the GAUSSIAN-98 program package [13]. The ^{119}Sn Mössbauer nuclear quadrupole splitting was calculated by the calibration formula $\Delta_{calcd} = 0.93 \cdot V \pm 0.58$ mm s^{-1} [12], where

Table 1

Analytical data [calculated % values in parentheses] of $(R_2Sn)_2MCl_n$[meso-tetra(4-sulfonatophenyl)porphinate] and $(R_3Sn)_4MCl_n$[meso-tetra(4-sulfonatophenyl)porphinate] (M = Fe(III), Mn(III): $n = 1$, R = Me, n-Bu, Ph; M = Sn(IV): $n = 2$, R = Me, n-Bu)

Compound[a]	C	H	N	S	H$_2$O
$(Me_2Sn)_2FeClTPPS \cdot 6H_2O$	40.73 (40.43)	3.14 (3.39)	3.35 (3.93)	8.46 (9.00)	7.82 (7.56)
$(n\text{-}Bu_2Sn)_2FeClTPPS \cdot 6H_2O$	45.02 (45.20)	4.96 (4.55)	3.50 (3.51)	7.56 (8.05)	7.31 (6.97)
$(Ph_2Sn)_2FeClTPPS \cdot 6H_2O$	48.30 (48.79)	3.64 (3.37)	3.17 (3.35)	7.08 (7.66)	7.05 (6.45)
$(Me_3Sn)_4FeClTPPS \cdot 6H_2O$	37.55 (37.71)	4.24 (4.07)	3.25 (3.14)	7.11 (7.19)	7.00 (6.06)
$(n\text{-}Bu_3Sn)_4FeClTPPS \cdot 6H_2O$	49.83 (48.28)	6.60 (6.34)	2.49 (2.45)	5.79 (5.61)	4.63 (4.72)
$(Ph_3Sn)_4FeClTPPS \cdot 6H_2O$	57.26 (55.10)	3.34 (3.83)	2.51 (2.22)	5.39 (5.07)	5.01 (4.27)
$(Me_2Sn)_2MnClTPPS \cdot 6H_2O$	39.87 (40.46)	3.96 (3.40)	4.10 (3.93)	8.43 (9.00)	7.28 (7.58)
$(n\text{-}Bu_2Sn)_2MnClTPPS \cdot 6H_2O$	44.76 (45.23)	4.57 (4.55)	3.71 (3.52)	7.88 (8.05)	6.78 (6.11)
$(Ph_2Sn)_2MnClTPPS \cdot 6H_2O$	48.99 (48.81)	3.77 (3.37)	3.23 (3.35)	7.72 (7.67)	6.85 (6.45)
$(Me_3Sn)_4MnClTPPS \cdot 6H_2O$	38.33 (37.73)	4.34 (4.07)	3.53 (3.14)	7.32 (7.20)	6.06 (6.54)
$(n\text{-}Bu_3Sn)_4MnClTPPS \cdot 6H_2O$	49.23 (48.30)	5.51 (6.34)	3.71 (2.45)	7.65 (5.61)	4.43 (4.72)
$(Ph_3Sn)_4MnClTPPS \cdot 6H_2O$	54.38 (55.12)	3.97 (3.82)	2.41 (2.22)	4.76 (5.08)	5.50 (4.27)
$(Me_2Sn)_2SnCl_2TPPS \cdot 6H_2O$	37.19 (37.82)	3.29 (3.17)	3.57 (3.67)	8.80 (8.41)	6.98 (7.09)
$(n\text{-}Bu_2Sn)_2SnCl_2TPPS \cdot 6H_2O$	43.15 (42.58)	4.30 (4.28)	3.26 (3.31)	7.90 (7.58)	6.41 (6.63)
$(Me_3Sn)_4SnCl_2TPPS \cdot 6H_2O$	34.92 (35.74)	3.56 (3.85)	2.77 (2.97)	6.61 (6.81)	6.02 (5.74)

[a] FeClTPPS^{4-} = Fe(III)Cl[meso-tetra(4-sulfonatophenyl)porphinate]$^{4-}$; MnClTPPS^{4-} = Mn(III)Cl[meso-tetra(4-sulfonatophenyl)porphinate]$^{4-}$; SnCl$_2$TPPS^{4-} = Sn(IV)Cl$_2$[meso-tetra(4-sulfonatephenyl)porphinate]$^{4-}$.

Table 2

Relevant absorption bands of Me$_3$SnSO$_3$R[a] (R = CH$_3$,CF$_3$), H$_4$MCl$_n$[*meso*-tetra(4-sulfonatophenyl)porphinate], (R$_2$Sn)$_2$MCl$_n$[*meso*-tetra(4-sulfonatophenyl)porphinate] and (R$_3$Sn)$_4$MCl$_n$[*meso*-tetra(4-sulfonatophenyl)porphinate] derivatives [(M = Fe(III), Mn(III); n = 1; R = Me, *n*-Bu, Ph), (M = Sn(IV), n = 2, R = Me, *n*-Bu)] in the 4000–250 cm^{-1} region[b]

Compounds[c]/assignment	v(SO$_3$) (A″)	v(SO$_3$) (A′)	v(SO$_3$) (A′)	v(SO$_3$) (A″)	v(SO$_3$) (A′)	v(SO$_3$) (A′)	ρ(SO$_3$) (A″)	ρ(SO$_3$) (A′)	Y-mode
Me$_3$SnSO$_3$CH$_3$	1266s	1112vs	1035s	562s	531s	516ms	352m,sh 346m,sh	275m,sh	
Me$_3$SnSO$_3$CF$_3$	1319vs	1145s	1026s	633s	577ms	530m,sh	356ms 347s	317m	
H$_4$FeClTPPS	1203s	1123s	1034vs	577s	n.o.	n.o.			
(Me$_2$Sn)$_2$FeClTPPS · 6H$_2$O	1202s	1121s	1035vs	579s	549w	520w	371w 342w	285w	
(*n*-Bu$_2$Sn)$_2$FeClTPPS · 6H$_2$O	1203s	1119s	1033vs	580s	548w	522w	370w 341w	281w	
(Ph$_2$Sn)$_2$FeClTPPS · 6H$_2$O	1203s	1121s	1034vs	579s	551w	525w	368w 341w	284w	450m
(Me$_3$Sn)$_4$FeClTPPS · 6H$_2$O	1202m	1121s	1036vs	580w	553m	521w	363w 337w	279w	
(*n*-Bu$_3$Sn)$_4$FeClTPPS · 6H$_2$O	1203m	1118s	1035vs	579m	551w	521w	364w 337w	283w	
(Ph$_3$Sn)$_4$FeClTPPS · 6H$_2$O	1202m	1112s	1034vs	579w	549m	520w	370m 341w	280w	453m
H$_4$MnClTPPS	1206	1123	1035	578	551	526			
(Me$_2$Sn)$_2$MnClTPPS · 6H$_2$O	1205m	1121s	1035vs	580s	548w	523w	355w 335w	275m	
(*n*-Bu$_2$Sn)$_2$MnClTPPS · 6H$_2$O	1206m	1119s	1034vs	579s	550w	525w	346w 330w	272m	
(Ph$_2$Sn)$_2$MnClTPPS · 6H$_2$O	1206m	1122s	1035vs	579s	550m	522w	350w 330s	270m	451m
(Me$_3$Sn)$_4$MnClTPPS · 6H$_2$O	1205m	1124s	1036vs	579s	551m	523w	350w 335w	276w	
(*n*-Bu$_3$Sn)$_4$MnClTPPS · 6H$_2$O	1206s	1119s	1035vs	580s	550w	520w	349w 330w	270w	
(Ph$_3$Sn)$_4$MnClTPPS · 6H$_2$O	1205m	1118s	1035vs	580s	550w	526w	350w 330s	273m	453m
H$_4$SnCl$_2$TTPS	1215m,bd	1124m	1033s	577m	548w	n.o			
(Me$_2$Sn)$_2$SnCl$_2$TPPS · 6H$_2$O	1214s	1123s	1036s	579s	550w	520w	390w 380w	280w	
(*n*-Bu$_2$Sn)$_2$SnCl$_2$TPPS · 6H$_2$O	1212s	1123s	1035s	580m	550w	520w	385w 375w	290w	
(Me$_3$Sn)$_4$SnCl$_2$TPPS · 6H$_2$O	1210s	1124s	1036s	581m	550s	530w	385w 375vw	290vw	

[a] See Ref. [14].

[b] s = Strong, m = medium, w = weak, sh = shoulder, bd = broad, v = very, n.o. = not observed.

[c] FeClTPPS^{4-} = Fe(III)Cl[*meso*-tetra(4-sulfonatophenyl)porphinate]$^{4-}$; MnClTPPS^{4-} = Mn(III)Cl[*meso*-tetra(4-sulfonatophenyl)porphinate]$^{4-}$, SnCl$_2$-TPPS^{4-} = Sn(IV)Cl$_2$[*meso*-tetra(4-sulfonatophenyl)porphinate]$^{4-}$.

$$V = V_{zz}\left[1 + \frac{1}{3}\left(\frac{V_{xx} - V_{yy}}{V_{zz}}\right)^2\right]^{1/2},$$

and where V_{xx}, V_{yy}, V_{zz}, following the condition $|V_{zz}| \geqslant |V_{yy}| \geqslant |V_{xx}|$, are the eigenvalues of the diagonalized electric field gradient tensor, calculated at the same level of theory of the higher layer.

3. Results and discussion

3.1. IR spectra

According to the literature reports, the ionic sulfonate group RSO$_3^-$, C_{3v} symmetry, should present in its IR spectrum six fundamental vibrations, three of which should be A′ and three doubly degenerate E modes [14]. Coordination of the sulfonate group RSO$_3^-$ should decrease the symmetry to C_s, removing in this way the degeneracy of the E mode vibrations. As a consequence, the coordinated sulfonate group should originate six A′ and three A″ vibrational modes. The infrared data of all the newly synthesized complexes, (R$_2$Sn)$_2$MCl$_n$[*meso*-tetra(4-sulfonatophenyl)porphinate]s and (R$_3$Sn)$_4$MCl$_n$[*meso*-tetra(4-sulfonatophenyl)porphinate]s showed the occurrence of the nine expected S–O vibrations, Table 2, which, according to previous reports [6,14–19], may be attributed to a monoanionic mono or bidentate binding of the sulfonate groups. These findings would support a six coordination around the tin(IV) atom in the (R$_2$Sn)$_2$MCl$_n$[*meso*-tetra(4-sulfonatophenyl) porphinate] complexes, with *trans*-R$_2$ octahedral configuration, possibly in a polymeric configuration. Four or five coordination, the latter with a monomeric bidentate

Table 3
Experimental Mössbauer parameters, isomer shift, δ, mm s^{-1}, and nuclear quadrupole splittings, $|\Delta_{exp}|$, mm s^{-1}, of H$_4$Fe(III)Cl[*meso*-tetra(4-sulfonatophenyl)porphine], H$_4$Sn(IV)Cl$_2$[*meso*-tetra(4-sulfonatophenyl)porphine], (R$_2$Sn)$_2$MCl$_n$[*meso*-tetra(4-sulfonatophenyl)porphinate], (R$_3$Sn)$_4$MCl$_n$-[*meso*-tetra(4-sulfonatophenyl)porphinate], [(M = Fe(III), Mn(III), n = 1, R = Me, *n*-Bu, Ph); (M = Sn(IV), n = 2, R = Me, *n*-Bu)], measured at liquid N$_2$ temperature

Compounds[a]	δ_{Sn}[b] (mm s^{-1})	$|\Delta_{exp}|$[b] (mm s^{-1})	δ_{Fe}[c] (mm s^{-1})	$|\Delta_{exp}|$[c] (mm s^{-1})
H$_4$Fe(III)ClTPPS			0.23	0.34
(Me$_2$Sn)$_2$FeClTPPS · 6H$_2$O	1.36	4.29	0.24	0.32
(*n*-Bu$_2$Sn)$_2$FeClTPPS · 6H$_2$O	1.52	4.74	0.22	0.36
(Ph$_2$Sn)$_2$FeClTPPS · 6H$_2$O	1.20	3.70	0.25	0.36
(Me$_3$Sn)$_4$FeClTPPS · 6H$_2$O	1.41	3.94	0.23	0.32
(*n*-Bu$_3$Sn)$_4$FeClTPPS · 6H$_2$O	1.52	4.08	0.23	0.36
(Ph$_3$Sn)$_4$FeClTPPS · 6H$_2$O	1.30	3.52	0.20	0.33
	δ_{Sn}[b] (mm s^{-1})	$|\Delta_{exp}|$[b] (mm s^{-1})	δ_{Sn}[b] (mm s^{-1})	$|\Delta_{exp}|$[b] (mm s^{-1})
(Me$_2$Sn)$_2$MnClTPPS · 6H$_2$O	1.46	4.29		
(*n*-Bu$_2$Sn)$_2$MnClTPPS · 6H$_2$O	1.54	4.64		
(Ph$_2$Sn)$_2$MnClTPPS · 6H$_2$O	1.37	3.70		
(Me$_3$Sn)$_4$MnClTPPS · 6H$_2$O	1.32	3.39		
(*n*-Bu$_3$Sn)$_4$MnClTPPS · 6H$_2$O	1.56	4.23		
(Ph$_3$Sn)$_4$MnClTPPS · 6H$_2$O	1.33	3.39		
H$_4$SnCl$_2$TPPS			0.27	1.04
(Me$_2$Sn)$_2$SnCl$_2$TPPS · 6H$_2$O	1.36	4.06	0.27	1.07
(Bu$_2$Sn)$_2$SnCl$_2$TPPS · 6H$_2$O	1.54	4.16	0.27	1.04
(Me$_3$Sn)$_4$SnCl$_2$TPPS · 6H$_2$O	1.45	3.53	0.27	1.04

[a] FeClTPPS^{4-} = Fe(III)Cl[*meso*-tetra(4-sulfonatophenyl)porphinate]$^{4-}$; MnClTPPS^{4-} = Mn(III)Cl[*meso*-tetra(4-sulfonatophenyl)porphinate]$^{4-}$; SnCl$_2$-TPPS^{4-} = Sn(IV)Cl$_2$[*meso*-tetra (4-sulfonatophenyl)porphinate]$^{4-}$; sample thickness ranged between 0.50 and 0.60 mg ^{119}Sn cm^{-2}.
[b] Isomer shift, $\delta \pm 0.03$ mm s^{-1} with respect to RT BaSnO$_3$; nuclear quadrupole splittings, $|\Delta| \pm 0.02$ mm s^{-1}.
[c] Isomer shift, $\delta \pm 0.03$ mm s^{-1} with respect to RT enriched ^{57}Fe foil (^{57}Fe = 95.2%); nuclear quadrupole splittings, $|\Delta| \pm 0.02$ mm s^{-1}.

or a polymeric monodentate trigonal bipyramidal environment around the tin(IV) atom, may be invoked for the (R$_3$Sn)$_4$MCl$_n$[*meso*-tetra(4-sulfonatophenyl)porphinate] complexes.

Furthermore, the Sn–Ph Y-mode of Whiffen [20] was present at around 450 cm^{-1} for (Ph$_2$Sn)$_2$MCl$_n$[*meso*-tetra-(4-sulfonatophenyl)porphinate]s and (Ph$_3$Sn)$_4$MCl$_n$-[*meso*-tetra(4-sulfonatophenyl)porphinate]s. As far as v(SnCl) stretching frequency related to the central SnCl$_2$ moieties in organotin-SnCl$_2$[*meso*-tetra(4-sulfonatophenyl)porphinate]s (ranging from 300 to 310 cm^{-1}), the frequency is comparable with the reported value of 309 cm^{-1} for SnCl$_2$[tetra-*p*-tolylporphyrin] [21].

3.2. ^{57}Fe and ^{119}Sn Mössbauer spectra

Both ^{57}Fe and ^{119}Sn Mössbauer spectroscopies have been applied to (R$_2$Sn)$_2$Fe(III)Cl[*meso*-tetra(4-sulfonatophenyl)porphinate]s and to (R$_3$Sn)$_4$Fe(III)Cl[*meso*-tetra(4-sulfonatophenyl)porphinate]s (Table 3, Fig. 2a and b), while only ^{119}Sn Mössbauer spectroscopy has been used to investigate (R$_2$Sn)$_2$Mn(III)Cl[*meso*-tetra(4-sulfonatophenyl)porphinate]s, (R$_3$Sn)$_4$Mn(III)Cl[*meso*-tetra(4-sulfonatophenyl)porphinate]s, (R$_2$Sn)$_2$Sn(IV)Cl$_2$[*meso*-tetra(4-sulfonatophenyl)-porphinate]s and, finally, (R$_3$Sn)$_4$Sn(IV)-Cl$_2$[*meso*-tetra(4-sulfonatophenyl)porphinate]s (Table 3).

The isomer shifts, δ (mm s^{-1}) and the experimental nuclear quadrupole splittings, $|\Delta_{exp}|$ (mm s^{-1}), measured with ^{57}Fe Mössbauer spectroscopy, both for the free Fe(III)ClH$_4$[*meso*-tetra(4-sulfonatophenyl)porphine], and for all its organotin(IV) derivatives, (R$_2$Sn)$_2$Fe(III)Cl-

[*meso*-tetra(4-sulfonatophenyl)porphinate]s and (R$_3$Sn)$_4$-Fe(III)Cl[*meso*-tetra(4-sulfonatophenyl)porphinate]s, are characteristic of Fe(III) $S = 5/2$ compounds [22]. The invariance of δ, on going from the free Fe(III)ClH$_4$[*meso*-tetra(4-sulfonatophenyl)porphine] to the complexes, shows that the ^{57}Fe Mössbauer parameter δ is independent from the withdrawing or releasing electronic effects of the organotin(IV) moieties coordinated to the side chain sulfonate groups. On the other hand, according to previous reports [23], both (R$_2$Sn)$_2$Fe(III)Cl[*meso*-tetra(4-sulfonatophenyl)porphinate] and (R$_3$Sn)$_4$Fe(III)Cl[*meso*-tetra(4-sulfonatophenyl)porphinate] complexes which possess, compared to the free Fe(III)ClH$_4$[*meso*-tetra(4-sulfonatophenyl)porphine], methyl and butyl electron-releasing substituents, should have larger Δ values. Table 3 also shows that, for the investigated complexes, the ^{57}Fe $|\Delta_{exp}|$ values vary, with respect to the free Fe(III)ClH$_4$[*meso*-tetra(4-sulfonatophenyl)porphine], within the experimental errors.

An asymmetric distribution of the electron charges around the ^{57}Fe, gives a non-zero electric field gradient.

According to the $|\Delta_{exp}|$ values obtained (Table 3), it is possible to hypothesize that the side chain organotin(IV) moieties do not influence neither the lattice contribution, q_{lat}, arising from the four endocyclic nitrogen atoms of the porphyrin ring and from the chloride directly bonded to the iron(III) center, nor the valence contributions, q_{val}, resulting from the asymmetric distribution of electrons in the bonding and non-bonding orbitals and in particular from the effective population of the 3d and 4p orbitals of the Fe(III) [24].

As far as ^{119}Sn Mössbauer data are concerned, the trend of the isomer shift values of the complexes, δ,
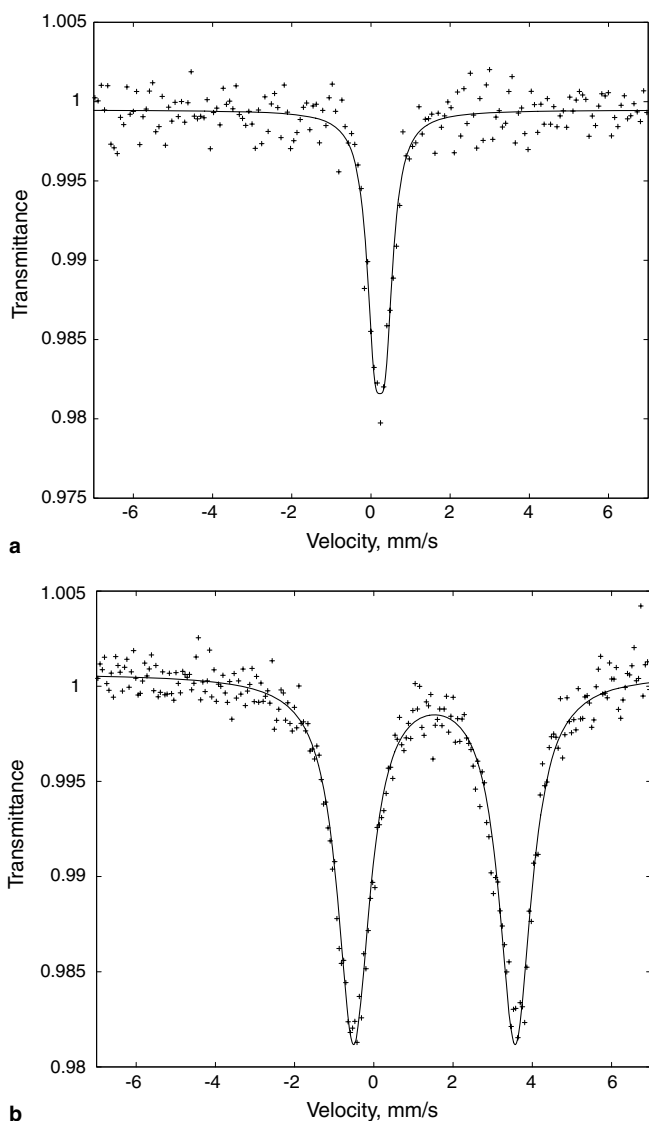
present in the organotin(IV)MCl$_n$[*meso*-tetra(4-sulfonatophenyl)porphinate]s, results in smaller nuclear quadrupole splittings, see Table 3.

A typical Mössbauer spectrum for (Me$_3$Sn)$_4$Sn(IV)-Cl$_2$TPPS is reported in Fig. 3 in which the contribution of the inorganic tin(IV) ($|\Delta_{exp}| = 1.04$ mm s^{-1}) and of the triorganotin(IV) moieties ($|\Delta_{exp}| = 3.53$ mm s^{-1}) are visible, characteristic of eq-R$_3$ trigonal bipyramidal geometry, Fig. 4c).

In conclusion, according both to IR and Mössbauer findings, polymeric octahedral *trans*-R$_2$Sn configurations are proposed, for diorganotin(IV)M(III)Cl[*meso*-tetra(4-sulfonatophenyl)porphinate]s (Fig. 4a and b), and polymeric trigonal bipyramidal equatorial R$_3$Sn for triorganotin(IV)-M(III)Cl[*meso*-tetra(4-sulfonatophenyl)porphinate]s (Fig. 4c).

In the structures shown in Fig. 4a and b, the formal charge 2+ of each of two diorganotin(IV) moieties is counterbalanced by the total 4− charge of four bridging or of two chelating monoanionic sulfonate groups. In both cases, the coordination polyhedron of tin(IV) should be formed by four equatorial oxygen atoms and two *trans*-R$_2$ groups. In the latter case, equal bonding situation should be envisaged for each of the four sulfonate groups of the porphine ligand, thus giving origin to a complex polymeric structure, where all the diorganotin(IV) groups should be inter-connected by two bridging sulfonate groups, belonging to two different [*meso*-tetra(4-sulfonatophenyl) porphinate] molecules.

A similar structure should be hypothesized also for the triorganotin(IV) complexes, where, however, there should be only one sulfonate bridge between each pair of metal atoms, and two of such bridges for each triorganotin(IV) moiety, counterbalancing the formal +1 charge on the tin(IV) atom. The coordination polyhedron of the tin(IV) atom should be a trigonal bipyramid with equatorial SnC$_3$ units and two axial oxygen atoms, from two sulfonate groups belonging to two different ligand molecules.

Fig. 2. (a) ^{57}Fe Mössbauer spectrum of (*n*-Bu$_3$Sn)$_4$FeClTPPS · 6H$_2$O. (b) ^{119}Sn Mössbauer spectrum of (*n*-Bu$_3$Sn)$_4$FeClTPPS · 6H$_2$O.

reflected the meaning of the parameter, increasing from methyl to butyltin(IV)MCl$_n$[*meso*-tetra(4-sulfonatophenyl)-porphinate] derivatives and decreasing in phenyltin-(IV)MCl$_n$[*meso*-tetra(4-sulfonatophenyl)porphinate], M = Fe(III), Mn(III). This trend, according to the literature reports [25–27], reflects the difference in number and electronegativity of the organic radicals bonded to the tin(IV) atom. In Table 3 are reported, for comparison purpose, the isomer shifts of several tin and organotin sulfonate complexes, previously reported in the literature [14–18], from which it is possible to evidence the covalent character [14] of the bonds in the complexes reported in this paper.

The electronegativity of the SO$_3$ groups in MCl$_n$-[*meso*-tetra(4-sulfonatophenyl)porphinate]$^{4-}$, M = Fe(III), Mn(III), Sn(IV) according to Yeats et al. [16], causes a withdrawal of p-electron density of the tin in organotin(IV) moieties, with concomitant deshielding of the tin 5s electrons, resulting in the δ values observed. Additionally, the above mentioned imbalance in the p orbital charge

Fig. 3. ^{119}Sn Mössbauer spectrum of (Me$_3$Sn)$_4$SnCl$_2$TPPS · 6H$_2$O.
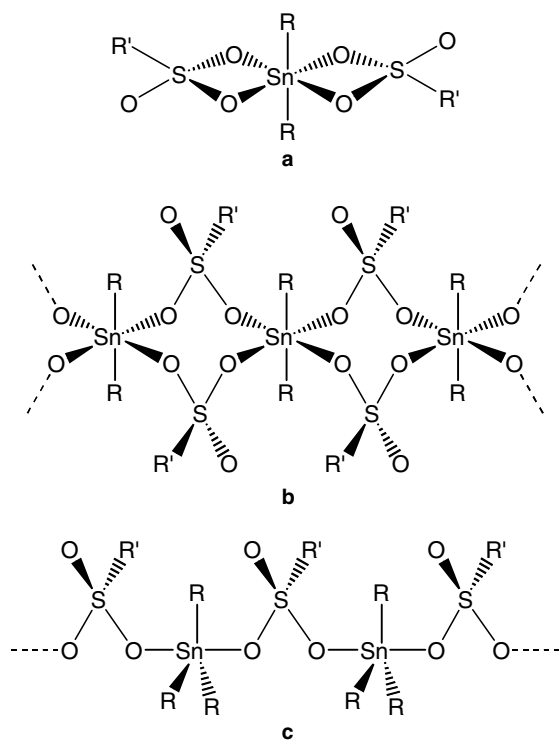
Fig. 4. Proposed octahedral polymeric configurations for $(R_2Sn)_2$-MCl_n[meso-tetra(4-sulfonatophenyl)porphinate], (a and b), through chelating (a) or bridging (b) sulfonate groups coordinating in the equatorial plane, and trigonal bipyramidal polymeric configuration for $(R_3Sn)_4MCl_n$[meso-tetra(4-sulfonatophenyl)porphinate] (c), [M = Fe(III), Mn(III), $n = 1$, R = Me, n-Bu, Ph; M = Sn(IV), $n = 2$, R = Me, n-Bu; R' = meso-tris(3-sulfonatophenyl)porphinate].

3.3. Quantum chemical calculations

The experimental ^{119}Sn $|\Delta|$ values obtained for the triorganotin(IV) moieties coordinated by the [meso-tetra(4-sulfonatophenyl)porphinate] derivative ligands (Table 3) are typical of tbp structures [28]. This leads to two possible structural hypotheses for the tin environment of these peripheral organotin groups: (i) a monomeric monodentate coordination or (ii) a polymeric bidentate coordination of the phenylsulfonate groups (see Fig. 4c). On the other hand, the ^{119}Sn $|\Delta_{exp}|$ values observed for the diorganotin(IV) moieties in analogous systems (Table 3) are typical of trans-R_2 octahedral coordination [28] and, considering the stoichiometry of such systems, could be well contemplated by a polymeric chelating bidentate or bridging coordination of the phenylsulfonate groups (see Fig. 4a and b).

To rationalize these structural hypotheses on the tin coordination environment, inferred on the basis of the spectroscopic evidences obtained for the investigated compounds, quantum chemical calculations have been performed on the model systems shown in Fig. 5a–c. The relevant structural data of the optimized geometries are reported in Table 4, while the corresponding calculated ^{119}Sn Δ values are reported in Table 5.

The first system considered (Fig. 5a) mimics a monomeric tbp coordination of the complex $(Me_3Sn)_4SnCl_2$-

[meso-tetra(4-sulfonatophenyl)porphinate]. Moreover, this model allows us to get detailed information of the structure of the $SnCl_2$ moiety coordinated by the porphyrin nitrogen atoms. The results obtained show that the $SnCl_2$ group, within the porphyrin plane, lies in a regular octahedral structure, analogously to what observed in $Sn(IV)Cl_2H_4$-[meso-tetra(4-sulfonatophenyl)porphinate].

Concerning the peripheral $Me_3Sn(IV)$ groups, the calculated parameters for the considered system (Table 4) allow us to conclude that their structure could be described as a tetrahedral environment, with a strong Sn2–O1 and an additional weak Sn2–O2 bond, distorted towards a trigonal bipyramidal configuration in analogy to what observed for $(Me_3Sn)_4H_2$[meso-tetra(4-sulfonatophenyl)porphinate].

To mimic the possible polymeric coordination of the $Me_3Sn(IV)$ moieties by the sulfonate groups of two different [meso-tetra(4-sulfonatophenyl)porphinate] derivative ligands, the structure shown in Fig. 5b was considered as model system. It turns out that the sulfonate groups would act, in this case, as monodentate axial ligands with the methyl groups in the equatorial plane of a distorted tbp structure (see Table 4). For both the monomer and polymer model systems, reported in Fig. 5a–c there is a good agreement between the calculated nuclear quadrupole splitting value and the corresponding experimental value obtained for $(Me_3Sn)_4SnCl_2$[meso-tetra(4-sulfonatophenyl)porphinate] (Table 5). However, the occurrence of Mössbauer effect at room temperature for $(Me_3Sn)_4SnCl_2$[meso-tetra(4-sulfonatophenyl)porphinate] would induce us to preferably attribute the polymeric structure reported in Fig. 5b for the triorganotin(IV) complexes of the [meso-tetra(4-sulfonatophenyl)porphinate] derivatives investigated.

We mention that any attempt to optimize the dimethyltin(IV)-phenylsulfonate coordination geometry in the environment proposed in Fig. 4b failed, essentially as a consequence of a strong steric repulsion between the vicinal R' groups.

On the other hand, the system considered in Fig. 5c mimics a polymeric trans-Me_2 octahedral coordination of the tin atom in the $(Me_2Sn)_2SnCl_2$[meso-tetra(4-sulfonatophenyl)porphinate] complex. The structural parameters obtained (Table 4) show that this structure can be described as a distorted trans-Me_2 octahedron, with a quite small C–Sn–C bond angle, and with an asymmetric chelation of the sulfonate groups to the tin atom. The very good agreement between the experimental and the calculated ^{119}Sn Δ values (Table 5) allow us to suggest the proposed structural attribution for the organotin(IV) complexes of the investigated derivatives.

3.4. ^1H and ^{13}C NMR spectra of diorganotin(IV) and triorganotin(IV)[meso-tetra(4-sulfonatophenyl)-porphinatetin(IV)dichloride] complexes

^1H and ^{13}C NMR spectra of aqueous (D_2O) solutions of non-paramagnetic complexes have been investigated. Caution must be exercised in interpreting NMR spectra of
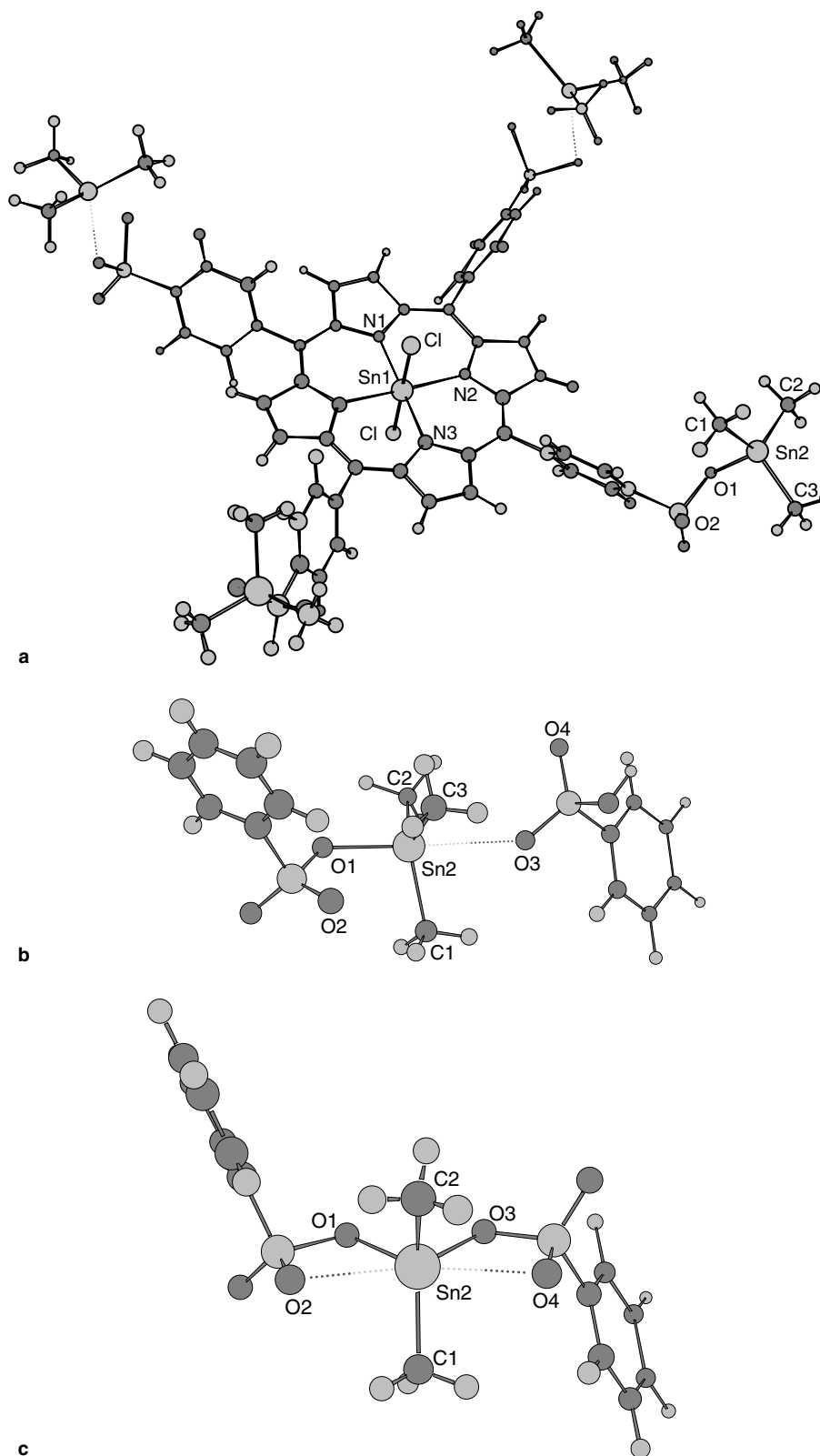
Fig. 5. Optimized structures (see text) of the monomeric $(Me_3Sn)_4SnCl_2TPPS$ complex (a), and of $Me_3Sn(PS)(HPS)$ (b) and $Me_2Sn(PS)_2$ (c), the latter two being models of the polymeric complexes of di- and trimethyltin(IV)-TPPS.

meso-tetra(4-sulfonatophenyl)porphine (H_6TPPS), metalloporphine derivative $SnCl_2H_4TPPS$ and its organometallic complexes reported in this work, since they appear to be

dependent on experimental conditions such as concentration, temperature and solvent; moreover the use of DSS [3-(trimethylsilyl)-1-propanesulfonic acid sodium salt], as

Table 4
Relevant geometrical parameters (bond distances/Å and angles/°) relative to the tin environment in the higher layer of the systems shown in Fig. 5a–c, calculated at DFT level by the ONIOM method (see text)

	$(Me_3Sn)_4SnCl_2TPPS$	$Me_3Sn(PS)(HPS)$	$Me_2Sn(PS)_2$
Sn1–Cl	2.47	–	–
Sn1–N	2.13	–	–
Cl–Sn1–Cl	180	–	–
N1–Sn1–N2	90	–	–
N1–Sn1–N3	180	–	–
Cl–Sn1–N	90	–	–
Sn2–C	2.16	2.17	2.15
Sn2–O1	2.12	2.15	2.14
Sn2–O2	3.19	3.29	2.72
Sn2–O3	–	2.96	2.14
Sn2–O4	–	4.65	2.72
O1–Sn2–O2	51	49	58
O1–Sn2–O3	–	173	84
O1–Sn2–O4	–	146	142
C1–Sn2–C2	115	117	135
C1–Sn2–C3	117	118	–
C2–Sn2–C3	115	117	–
O1–Sn2–C1	105	101	106
O1–Sn2–C2	96	94	107
O1–Sn2–C3	105	102	–
O2–Sn2–C1	78	80	86
O2–Sn2–C2	147	80	87
O2–Sn2–C3	81	83	–

HPS = phenylsulfonic acid; $SnCl_2TPPS^{4-}$ = Sn(IV)Cl$_2$[*meso*-tetra(4-sulfonatophenyl)porphinate]$^{4-}$;
Sn1 is the tin atom of the $SnCl_2TPPS^{4-}$ anion; Sn2 is the tin atom of the organotin moiety (Fig. 5a–c).

Table 5
^{119}Sn Mössbauer nuclear quadrupole splitting (Δ, mm s^{-1}), relative to the indicated tin atom, calculated (see text) for the compounds shown in Fig. 5a–c, and compared to the corresponding experimental values obtained for $(Me_2Sn)_2SnCl_2TPPS \cdot 6H_2O$ and $(Me_3Sn)_4SnCl_2TPPS \cdot 6H_2O$ (see Table 3)

Compound[a]	Tin atom[b]	$|\Delta_{exp}|$	Δ_{calcd}
$(Me_3Sn)_4SnCl_2TPPS \cdot 6H_2O$	Sn(1)	1.04	0.82
$(Me_3Sn)_4SnCl_2TPPS \cdot 6H_2O$	Sn(2)	3.53	−3.49
$Me_3Sn(PS)(HPS)$	Sn(2)	3.53	−3.76
$Me_2Sn(PS)_2$	Sn(2)	4.06	3.94

[a] $SnCl_2TPPS^{4-}$ = Sn(IV)Cl$_2$[*meso*-tetra(4-sulfonatophenyl)porphinate]$^{4-}$; HPS = phenylsulfonic acid.
[b] Sn(1) is the tin atom of the $SnCl_2TPPS^{4-}$ anion; Sn(2) is the tin atom of the organotin moiety.

an internal reference was prevented by significant interactions, in D$_2$O solution, of all compounds and DSS, as previously found for H$_2$TPPS^{4-} salts [8]. While the organometallic moieties are attached to the porphyrin periphery, Sn(IV) atoms and axially coordinated chloride ions are present at the centre of porphyrin ring. The favorable chemical and NMR properties of tin(IV)-porphyrin complexes have enabled the generation of spectroscopic, mainly NMR; *cis*- and *trans*-influence series for oxygen bound axial ligands of widely differing base strengths.

Dihydroxo-5,10,15,20-tetraphenylporphyrinatotin(IV), [Sn(IV)(OH)$_2$TPP], has been investigated by ^{1}H and ^{13}C NMR, compared with Sn(IV)Cl$_2$TPP, where no high-field peak due to Sn(OH)$_2$ is observed [29]. For both complexes, satellites are observed flanking the β-pyrrole proton resonance, which are assigned to long-range coupling to the tin(IV) nucleus over four bonds. The X-ray structure of *meso*-tetraphenylporphyrinatotin(IV) complexes with chloride, water, hydroxide, benzoate, salicylate and acetylsalicilate as axial ligands has been reported [30,31] all complexes being monomeric with little structural variations within the TPP framework. *Cis*-influences in octahedral tin(IV)X$_2$ *meso*-tetraphenylporphyrin complexes have been evaluated and correlations between spectroscopic properties and the nature of axial ligands X have been discussed. The tin(IV)-proton coupling constants to the β-pyrrole protons decrease from 19.2 Hz (X = ClO$_4$) to 10.4 Hz (9.5 Hz according to Ref. [28]) (X = OH) while for X = Cl ^4J(Sn,H) = 15.2 Hz (15.5 according to Ref. [28]) [32–34]. Coupling constants for the oxygen bounds ligands correlate satisfactory with the basicity of the ligands, while the halides do not fit this relationship possibly due to the overall effect of π back-bonding from chlorine to tin, effectively "tightening" coordination to the tin(IV) nucleus as suggested by the authors (see Table 6).

The chemical shifts of the β-protons also depend on the nature of X and a similar dependence on ligand basicity is observed, with weaker bases causing downfield shifts (δ for OH < δ for Cl < δ for ClO$_4$).

A detailed study of the effect of axially bound anions on the electrochemistry and spectroelectrochemistry, including ^{1}H NMR, of tin(IV)X$_2$ *meso*-tetra-*p*-tolylporphyrin or *meso*-tetra-*m*-tolylporphyrin has been reported [21]. An agreement with previously reported pattern is found, since the Sn(IV)Cl$_2$ derivative has a larger coupling constant than its bromide, hydroxo and fluoride analogues.

The kinetics of consecutive second-order two-steps hydrolysis of dimethoxo(*meso*-tetra-*p*-tolylporphyrinato)-tin(IV) has also been studied in CDCl$_3$ [35].

We previously investigated the interaction of [*meso*-tetra(4-sulfonatophenyl)porphine with diorgano and triorgano(IV) moieties and configurations of the complexes in DMSO-d_6 have been reported [6], hence the ^{1}H and ^{13}C NMR spectra of the new complexes may offer evidence of the influence of both peripheral organotin(IV) and central Sn(IV) substitution. 10^{-3} M solutions in D$_2$O of the dimethyl- and trimethyltin(IV) complexes have been obtained, while nearly saturated solutions of (*n*-Butyl)$_2$-Sn(IV) derivative has been examined, giving broad poorly resolved NMR spectra for the latter. For the former complexes conductivity measurements, which agree with a 1:2 electrolyte, indicate the formation of diaqua species. ^4J(Sn,H) coupling constants involving ^{119}Sn and ^{117}Sn nuclei (natural abundances 8.6% and 7.6%, respectively) and β-pyrrole protons are reported in Table 1. Individual couplings to ^{119}Sn and ^{117}Sn were not resolved so average values are given. The protons of the *meso*-phenyl substituents appear in the spectrum as a AB system with typical vicinal coupling of ca. 8 Hz. Relative to the parent

Table 6
RT ^{1}H NMR data for diorganotin and triorganotin-Sn(IV)Cl$_2$TPPS (coupling constants are given in Hz; chemical shifts are relative to external DSS; $B_0 = 5.87$ T[a,b])

Assignment/compound	H$_6$TPPS	I	II	II[c]	III	IV
N–H	n.o.					
m-H	8.41d	8.30d	8.27d	8.19m	8.25d	8.24d
	^3J(H,H) 8.0	^3J(H,H) 8.3	^3J(H,H) 8.0		^3J(H,H) 8.0	^3J(H,H) 7.8
o-H	8.73d	8.47d	8.47d	8.33m	8.45d	8.45d
	^3J(H,H) 8.0	^3J(H,H) 8.3	^3J(H,H) 8.0		^3J(H,H) 8.0	^3J(H,H) 7.8
β-pyrrole	8.99	9.49t	9.46t	9.35t	9.42	9.29t
		^4J(Sn,H) 14.7	^4J(Sn,H) 14.7	^4J(Sn,H) 13.1	^4J(Sn,H) n.o.	^4J(Sn,H) 12.7
R$_n$Sn(IV)			0.83t	0.94t	1.24m,b	0.22t
			^2J(Sn,H) 95.6	^2J(Sn,H) 106	1.40m,b	^2J(Sn,H) 64.2
					1.86m,b	
CSnC angle			154	174		115

[a] H$_6$TPPS = *meso*-tetra(4-sulfonatophenyl)porphine; I = SnCl$_2$H$_4$TPPS; II = (Me$_2$Sn)$_2$SnCl$_2$TPPS · 6H$_2$O; III = (*n*-Bu$_2$Sn)$_2$SnCl$_2$TPPS · 6H$_2$O; IV = (Me$_3$Sn)$_4$SnCl$_2$TPPS · 6H$_2$O.
[b] Solvent D$_2$O; DSS external reference; abbreviations: n.o., not observed; *i*, ipso; *o*, ortho; *m*, meta; *p*, para.
[c] Solvent DMSO-d_6; TMS internal reference.

SnCl$_2$H$_4$TPPS, all complexes show only minor shifts in chemical shifts, while ^4J(Sn,H) are in all instances ca. 15 Hz, suggesting retention of central Sn(IV) diaqua moiety. Several authors [29,32–34] investigated by ^{1}H NMR Sn(OH)$_2$ porphyrins in CDCl$_3$ and the high field resonance at ca. 7.5 ppm assigned to Sn(OH)$_2$ resonance. Since the complexes presented in this work are not soluble in CDCl$_3$, the potential hydrolytically generated Sn–OH protons might be detected by ^{1}H NMR in DMSO-d_6 solutions of all hexahydrated complexes. No high field resonance due to hydroxo groups has been detected.

Since in the context of a study on the monomer–dimer equilibrium (homo-dimers) in D$_2$O solutions of H$_2$TPPS^{4-} and its Zn^{2+} and Cu^{2+} complexes [8] it was shown that, even for concentrations as high as 0,044 mol dm^{-3}, in DMSO-d_6 the extent of aggregation of monomers is mini-

mal, the ^{1}H NMR spectrum of (Me$_2$Sn)$_2$SnCl$_2$H$_2$TPPS in this solvent at fixed 10^{-3} concentration, compared with the D$_2$O counterpart, could give some indication of formation of aggregates in D$_2$O. Following the formation of homo-aggregates, high field shifts are expected for β-pyrrole, ortho and meta protons, the β-pyrrolic signals being the ones which are shifted the most. Only minor high field shifts are observed, which may indicate that no major formation of aggregates has taken place. The C–Sn–C angle of 174° is probably due to the coordinating ability of DMSO towards the organometallic moieties.

The organometallic moieties in D$_2$O show coupling constants ^2J($^{117/119}$Sn,^{1}H) which may be related to the coordination polyhedron around tin atoms of the organometallic substituents, by use of the Lockhart and Manders equations [35].

Table 7
^{13}C NMR data for diorganotin and triorganotin SnCl$_2$[*meso*-tetra(4-sulfonatophenyl)porphinate] derivatives (coupling constants are given in Hz; chemical shifts are relative to external DSS; $B_0 = 5.87$ T[a,b])

Assignment/compound	H$_6$TPPS	I	I[c]	II	III	IV
C-*p*	149.69	149.4	148.96	149.6	149.7	149.5
C-α	145.33	145.5	147.41	145.6	146.2	145.8
C-*i*	139.21	145.2	139.05	145.5	145.7	145.6
C-*o*	138.66	137.6	137.71	137.8	137.9	137.9
		136.3				
C-β	128.61	^3J(Sn,C) 23	127.32	136.4	136.5	136.3
C-*m*	126.03	126.9	126.74	127.1	127.1	127.1
C-*meso*	121.78	123.3	122.86	123.5	n.o.	123.4
CH$_3$Sn				9.31		0.71
				^1J(Sn,C) 814		^1J(Sn,C) 479
					21.8	
					17.7	
CSnC angle				148		119

[a] H$_6$TPPS = *meso*-tetra(4-sulfonatophenyl)porphine; I = SnCl$_2$H$_4$TPPS; II = (Me$_2$Sn)$_2$SnCl$_2$TPPS · 6H$_2$O; III = (*n*-Bu$_2$Sn)$_2$SnCl$_2$TPPS · 6H$_2$O; IV = (Me$_3$Sn)$_4$SnCl$_2$TPPS · 6H$_2$O.
[b] Solvent D$_2$O; DSS external reference; abbreviations: n.o., not observed; *i*, ipso; *o*, ortho; *m*, meta; *p*, para.
[c] Solvent DMSO-d_6; TMS internal reference.

For $(Me_2Sn)_2SnCl_2TPPS$, C–Sn–C being 154°, this suggests retention of the distorted *trans* $Me_2Sn(IV)$ octahedral environment suggested for the complex in the solid state.

Similarly, for $(Me_3Sn)_4SnCl_2TPPS$, C–Sn–C being 115°, this suggests a distortion of the ideal trigonal-bipyramidal geometry of the polymeric solid complex. Relative to the ammonium derivative of H_2TPPS^{4-} in D_2O reported by Corsini [36], the ^1H NMR of H_6TPPS closely agrees with the pattern of resonances found at 100 °C by the authors and taken as an indication of minimal aggregation. The spectrum of $SnCl_2H_4TPPS$ presents, relative to H_6TPPS, a downfield shift of β-pyrrole resonance, due to insertion of electron withdrawing $Sn(IV)$ ion, while a minor high field shift of remaining aryl resonances is observed.

3.5. ^{13}C NMR spectra

For the dimethyl- and trimethyltin(IV)$SnCl_2TPPS$ complexes, whose solubility in D_2O enabled us to obtain 10^{-3} M solutions, typical seven-line spectra were observed, carbon resonances being assigned by chemical shift comparison with published literature (Table 7). C–Sn–C values, derived from the relevant equation [37], of 148° and 119°, respectively, closely agree with those obtained from ^1H NMR. (*n*-Butyl)$_2Sn(IV)$ derivative, being scarcely soluble in D_2O, afforded poorly resolved resonances which prevented evaluation of $^nJ(Sn,^{13}C)$.

$^3J(Sn,^{13}C)$ for β-carbons has been observed (23 Hz) for $SnCl_2H_4TPPS$ which agrees with the value (30.5 Hz) found in $CDCl_3$ by Milgrom and Sheppard for $SnCl_2TPP$ but not for $Sn(OH)_2TPP$ [29], while it was not discernible in the organometallic complexes. Resonances of all carbons in the organometallic complexes show only minor shifts relative to parent $SnCl_2H_4TPPS$, which supports the notion that coordination to peripheral sulfonato groups brings very little perturbation to the macrocycle diamagnetic ring current.

References

[1] L. Pellerito, A. Pellerito, F. Maggio, M. Beltramini, B. Salvato, F. Ricchelli, Appl. Organomet. Chem. 7 (1993) 79.
[2] R. Vitturi, L. Pellerito, E. Catalano, M.R. Lo Conte, Appl. Organomet. Chem. 7 (1993) 295.
[3] H. Brunner, F. Maiterth, B. Treittinger, Chem. Ber. 127 (1994) 2141.
[4] H. Yuan, L. Thomas, L.K. Woo, Inorg. Chem. 35 (1996) 2808.
[5] M.G. Mirisola, A. Pellerito, T. Fiore, G.C. Stocco, L. Pellerito, A. Cestelli, I. Di Liegro, Appl. Organomet. Chem. 11 (1997) 499.
[6] A. Pellerito, T. Fiore, A.M. Giuliani, F. Maggio, L. Pellerito, C. Mansueto, Appl. Organomet. Chem. 11 (1997) 707.
[7] E. Iengo, B. Milani, E. Zangrando, S. Geremia, E. Alessio, Angew. Chem. Int. Ed. 39 (2000) 1096.
[8] E. Alessio, E. Ciani, E. Iengo, V.Yu. Kukushkin, L.G. Marzilli, Inorg. Chem. 39 (2000) 1434.
[9] C. Pellerito, P. D'Agati, T. Fiore, C. Mansueto, V. Mansueto, G.C. Stocco, L. Nagy, L. Pellerito, J. Inorg. Biochem. 99 (2005) 1294.
[10] M.A. Costa, L. Pellerito, V. Izzo, T. Fiore, C. Pellerito, M. Melis, M.T. Musmeci, G. Barbieri, Cancer Lett. (2006) in press.
[11] S. Dapprich, I. Komáromi, K.S. Byun, K. Morokuma, M.J. Frisch, J. Mol. Struct. (Theochem) 462 (1999) 1.
[12] G. Barone, A. Silvestri, G. Ruisi, G. La Manna, Chem. Eur. J. 11 (2005) 6185.
[13] M.J. Frisch, G.W. Trucks, H.B. Schlegel, G.E. Scuseria, M.A. Robb, J.R. Cheeseman, V.G. Zakrzewski, J.A. Montgomery Jr., R.E. Stratmann, J.C. Burant, S. Dapprich, J.M. Millam, A.D. Daniels, K.N. Kudin, M.C. Strain, O. Farkas, J. Tomasi, V. Barone, M. Cossi, R. Cammi, B. Mennucci, C. Pomelli, C. Adamo, S. Clifford, J. Ochterski, G.A. Petersson, P.Y. Ayala, Q. Cui, K. Morokuma, D.K. Malick, A.D. Rabuck, K. Raghavachari, J.B. Foresman, J. Cioslowski, J.V. Ortiz, A.G. Baboul, B.B. Stefanov, G. Liu, A. Liashenko, P. Piskorz, I. Komaromi, R. Gomperts, R.L. Martin, D.J. Fox, T. Keith, M.A. Al-Laham, C.Y. Peng, A. Nanayakkara, M. Challacombe, P.M.W. Gill, B. Johnson, W. Chen, M.W. Wong, J.L. Andres, C. Gonzalez, M. Head-Gordon, E.S. Replogle, J.A. Pople, GAUSSIAN-98, Revision A.8, Gaussian, Inc., Pittsburgh, PA, 1998.
[14] P.A. Yeats, J.R. Sams, F. Aubke, Inorg. Chem. 10 (1971) 1877.
[15] R.J. Gillespie, E.A. Robinson, Can. J. Chem. 40 (1962) 644.
[16] P.A. Yeats, B.L. Poh, B.F.E. Ford, J.R. Sams, F. Aubke, J. Chem. Soc. (A) (1970) 191.
[17] H.A. Carter, S.P.L. Jones, F. Aubke, Inorg. Chem. 9 (1970) 2485.
[18] P.A. Yeats, J.R. Sams, F. Aubke, Inorg. Chem. 11 (1972) 2634.
[19] P.A. Yeats, B.F.E. Ford, J.R. Sams, F. Aubke, J. Chem. Soc., Chem. Commun. (1969) 791.
[20] D.H. Whiffen, J. Chem. Soc. (1956) 1350.
[21] J.C.S. Kadish, Q.Y.Y. Xu, G. Bhaskar Maiya, J.-M. Barbe, R. Guilard, J. Chem. Soc., Dalton Trans. (1989) 1531.
[22] J.R. Sams, T.B. Tsin, in: D. Dolphin (Ed.), The Porphyrins, Academic Press, New York, 1979.
[23] T. Ohya, M. Sato, J. Chem. Soc., Dalton Trans. (1996) 1519.
[24] R. Sternheimer, Phys. Rev. 130 (1963) 1423, and references therein.
[25] G.M. Bancroft, R.H. Platt, Adv. Inorg. Chem. Radiochem. 15 (1972) 59.
[26] N.N. Greenwood, T.C. Gibb, Mössbauer Spectroscopy, Chapman & Hall, London, 1971.
[27] K.C. Molloy, J.J. Zuckermann, H. Schumann, G. Rodewald, Inorg. Chem. 19 (1980) 1089.
[28] R.V. Parish, in: G.J. Long (Ed.), Mössbauer Spectroscopy Applied to Inorganic Chemistry, Plenum Press, New York, 1984.
[29] L.R. Milgrom, R.N. Sheppard, J. Chem. Soc., Chem. Commun. (1985) 350.
[30] D.M. Collins, W.R. Scheidt, J.L. Hoard, J. Am. Chem. Soc. 94 (1972) 6689.
[31] G. Smith, D.P. Arnold, C.H.L. Kennard, T.C.W. Mak, Polyhedron 10 (1991) 509.
[32] D.P. Arnold, Polyhedron 5 (1986) 1957.
[33] D.P. Arnold, Polyhedron 7 (1988) 2225.
[34] C.-C. Tsai, Y.-J. Chen, J.-H. Chen, L.-P. Hwang, Polyhedron 11 (1992) 1647.
[35] T.P. Lockhart, W.F. Manders, Inorg. Chem. 25 (1986) 892.
[36] A. Corsini, O. Herrmann, Talanta 33 (1986) 335.
[37] T.P. Lockhart, W.F. Manders, J.J. Zuckermann, J. Am. Chem. Soc. 107 (1985) 4546.